Linear spin-$\frac{1}{2}$ magnetic chains: Susceptibilities, correlation functions, and applications to $(C_6H_{11}NH_3)CuBr_3$ and deuterated $CuCl_2 \cdot 2(CH_3)_2SO$

G. Kamieniarz*
Instituut voor Theoretische Fysica, Katholieke Universiteit Leuven, B-3030 Leuven, Belgium
(Received 8 September 1987)

The susceptibilities, correlation functions, and correlation length of the spin-$\frac{1}{2}$ one-dimensional *XXZ* model are calculated for the chains with the finite size N and free boundary conditions. The infinite-chain results are estimated by extrapolation in $1/N$, and good convergence is found for most temperatures. Theoretical estimates are compared with the experimental results for the corresponding model compounds $C_6H_{11}NH_3CuBr_3$ (CHAB-d_{14}) and $CuCl_2 \cdot 2(CH_3)_2SO$ (CDC) in the deuterated versions. The crossover region of the in-plane correlation functions is revealed and the inverse correlation length is in a semiquantitative agreement with that measured for CHAB. The single-crystal magnetic susceptibility data for CDC are reinterpreted and the quantitative agreement with the experiment is found.

I. INTRODUCTION

One-dimensional (1D) magnetic systems have been the subject of great theoretical and experimental interest[1,2] in recent years. Their properties are usually described by the 1D anisotropic Heisenberg Hamiltonians with a given number of spin S. $(CD_3)_4NMnCl_3$ (Refs. 1–3) (TMMC) is known as a spin-$\frac{5}{2}$ quasi-one-dimensional antiferromagnet whereas $CsNiF_3$ (Refs. 1, 4, and 5) is a spin-1 compound with ferromagnetic intrachain interaction. A number of spin-$\frac{1}{2}$ systems has been found with both ferromagnetic[6–8] and antiferromagnetic interactions[9] which can be described by the Hamiltonian

$$H_0 = -2J\sum_i (S_i^x S_{i+1}^x + S_i^y S_{i+1}^y + \Delta S_i^z S_{i+1}^z) \ . \quad (1)$$

One of the best realizations of the 1D ferromagnetic model (1) is the compound $(C_6H_{11}NH_3)CuBr_3$ (CHAB). From various measurements[6,10] the parameters J and Δ have been established as

$$J/k_B = 55 \pm 5 \text{ K} \ , \quad \Delta = 0.95 \ .$$

The value of the corresponding g factor has been found from magnetization measurements[11]: $g = 2.01 \pm 0.02$.

The easy-plane Hamiltonian (1) with $\Delta < 1$ can be mapped[12] into a sine-Gordon (SG) Hamiltonian by having recourse to the continuum limit approximation, classical spin, and the limit of large anisotropy, confining the spins in the easy plane. In this context of nonlinear soliton excitations, the recent experiments[13] on CHAB in the presence of a magnetic field cannot be described quantitatively. The excess specific heat $\Delta C(H) = C(H) - C(H=0)$ measured experimentally does not cover one universal curve as it is predicted by the sine-Gordon (SG) theory.[14] Quantum corrections[15–20] implemented in the framework of the SG model turn out to be small. For CHAB they even result in larger deviations. The role of quantum effects has been enhanced within the semiclassical approach[21–22] but an agreement with experiment is still far from being quantitative.

Some attempts have been made to go beyond the SG approximation. The finite value of the anisotropy term in (1) leads to the out-of-plane motion of the spin. Neglecting quantum effects, the out-of-plane fluctuations have been taken into account in the numerical Monte Carlo[23] and transfer matrix[24,25] calculations. In contrast to the SG approach, the excess specific-heat data do not cover one universal curve, and the peak features are qualitatively correct. Recently a next step has been taken and both quantum as well as out-of-plane fluctuations have been taken into account in the theoretical calculations.[26,27] Two complementary numerical analyses of the anisotropic quantum Hamiltonian (1) have been put forward by having recourse to quantum Monte Carlo (QMC) and quantum transfer-matrix (QTM) calculations[26] and to extrapolation[27] of the finite-size results.

The quantum statistics applied to the model (1) does not yield the quantitative agreement with the experimental excess specific-heat $\Delta C(H)$ as far as the peak positions and peak heights are concerned. QMC and QTM results[26] support the conclusion that the experimental peak heights and positions for CHAB cannot be reproduced adequately for the acceptable value $(0.90 \le \Delta \le 0.96)$ of the easy-plane anisotropy parameter Δ. Independent finite-size calculations[27] confirm the disagreement between theory and experiment as far as peak positions are concerned. However, the peak-height predictions for the corresponding spin $S = \frac{1}{2}$ and $S = 1$ model Hamiltonians agree quantitatively with those of CHAB and $CsNiF_3$. For the $S = \frac{1}{2}$ Hamiltonian (1) the chains with size N up to 10 have been extrapolated to N infinite. This is a typical length of chains considered previously[28,29] in more simple zero-field cases for more symmetric interactions. These extrapolated (to infinite N) finite-size results are very well established. It was demonstrated that QMC results[30] and QTM results[31] converge towards those of Bonner and Fisher.[28] The QMC and QTM techniques

refer to the Trotter formalism[32] so that the one-dimensional quantum Hamiltonian is mapped onto a corresponding two-dimensional classical Hamiltonian on a strip. The length of the strip in the chain direction can exceed that considered in the finite-size technique by a factor 3 or more but in Trotter direction the length m is usually limited to $m=8$.

In this paper a numerical analysis of the quantum Hamiltonian (1) previously applied to the excess specific heat[27] is extended to other thermodynamic quantities. The correlation functions and the magnetic susceptibility are calculated by extrapolation of the corresponding finite-chain results. From the correlation function data the inverse correlation length is extracted. As concerns susceptibility, the results obtained here are compared with those known in the limit $\Delta=0$ (XY model[33]) and $\Delta=1$ (isotropic Heisenberg model[34]), and rather good agreement is revealed. A contact with the recent experiments on CHAB is made as far as the inverse correlation length is concerned. The semiquantitative agreement with experimental data is found for the standard choice of the parameters. In view of the reservations[26,27] on the applicability of the Hamiltonian (1) to CHAB, rather strong support in favor of this Hamiltonian is presented. In addition, the experimental susceptibility data on $CuCl_2\cdot 2[(CH_3)_2SO]$[9] (denoted as CDC) are reinterpreted in terms of the Hamiltonian (1).

The remainder of this paper is as follows. In Sec. II a brief description of the method and the zero-field results for the susceptibility, correlation functions, and the inverse correlation length are presented. Section III contains the comparison with recent experimental data and our concluding remarks.

II. METHOD AND THERMODYNAMIC FUNCTIONS

Here we are interested in zero-field results for the thermodynamic functions following the method applied previously[27] in the case of the field-dependent specific heat. Some calculations in zero field have already been performed[28,29] and the values given in (3) were inferred from the corresponding theoretical results and the specific-heat experimental data.[6]

We diagonalize numerically the corresponding matrices of the Hamiltonian (1) for finite chains with size N up to 11. Calculations are performed for chains with free ends in view of better convergence properties[29] and a truer representation[28] of the asymptotic ($N\rightarrow\infty$) shape for finite N. We are now able to consider longer chains then before,[27] since the higher symmetry now results in a reduction of the size of the matrices which must be diagonalized. For a given size N, the interesting thermodynamic quantities can be expressed in a standard way in terms of the eigenvalues E_i and the corresponding eigenvectors of the matrix representation (1). Having found the numerical data for these quantities, we can plot them versus the inverse length $1/N$ of the chains and extrapolate them to $N\rightarrow\infty$. As previously,[27] the scale $1/N$ is found to be appropriate for linear extrapolations. Many test calculations have been performed to check the program and the convergence. In particular, the zero-field specific-heat data[29] (Table IV) and some other data, reported in details below, have been fully recovered.

The accuracy of the extrapolations can be estimated by having recourse to the dispersion of the results when the number and size of chains used in the extrapolation procedure is changed. In general, the estimated uncertainties are implicitly indicated by the number of digits in the quoted data. Usually the error bars amount to 1 to 10 in the last digit, although the accuracy of some results is better since we report not more than five digits.

A. Correlation function results

We calculate the longitudinal and transverse zero-field spin pair correlation functions

$$\rho_z=\frac{1}{N}\left\langle\sum_{ij}\sigma_i^z\sigma_j^z\right\rangle=\langle(M^z)^2\rangle/N\ ,$$
$$\rho_x=\frac{1}{N}\left\langle\sum_{ij}\sigma_i^x\sigma_j^x\right\rangle=\langle(M^x)^2\rangle/N\ , \tag{2}$$

where $\sigma^{x,z}$ stand for the Pauli operators. To perform the calculations, we diagonalize the XXZ Hamiltonian (1) in the z representation. As the eigenvalues $\sigma=\sum_i\sigma_i$ of M^z are good quantum numbers, the size D of the diagonalized matrices can be reduced so that D does not exceed 462 for $N=11$. Finally, referring to the eigenvalues E_n and eigenvectors $|n\rangle$ of the Hamiltonian (1), the correlation functions (2) can be expressed by

$$\rho_{x,z}=\frac{1}{Z_0}\sum_n e^{-\beta E_n}\langle n|(M^{x,z})^2|n\rangle/N\ , \tag{3}$$

where Z_0 is the corresponding partition function.

The longitudinal correlation function ρ_z is related to the zero-field parallel susceptibility $\chi_\parallel$ defined as

$$\chi_\parallel=-\lim_{H\rightarrow 0}\left[\frac{\partial^2 F}{\partial H^2}\right]\ . \tag{4}$$

In the presence of the small longitudinal magnetic field H

$$\hat{H}=H_0-mHM^z \tag{5}$$

with H_0, M^z defined in (1) and (2), respectively, and $m=\frac{1}{2}g\mu_B$.

Using the Feynman identity

$$e^{-\beta(H_0+V)}=e^{-\beta H_0}T_\tau\left[\exp\left[-\int_0^\beta d\tau\, e^{\tau H_0}Ve^{-\tau H_0}\right]\right]\ , \tag{6}$$

where T_τ is the "time ordering" operator with respect to decreasing values of τ, the second term in (5) leads to the expansion

$$e^{-\beta(H_0+V)}=e^{-\beta H_0}\left[1-\int_0^\beta d\tau\, e^{\tau H_0}Ve^{-\tau H_0}+\int_0^\beta d\tau_1\int_0^{\tau_1}d\tau_2\, e^{\tau_1 H_0}Ve^{-(\tau_1-\tau_2)H_0}Ve^{-\tau_2 H_0}+\cdots\right]\ . \tag{7}$$

Commutativity of M^z and H_0 results in

$$Z(T,H)=\sum_n e^{-\beta E_n}[1-\beta mH\langle n \mid M^z \mid n\rangle + \tfrac{1}{2}(\beta mH)^2\langle n \mid (M^z)^2 \mid n\rangle + O(H^3)] , \tag{8}$$

so that

$$\chi_{\parallel}=N\beta m^2\rho_z \tag{9}$$

and we can make contact with some susceptibility data previously known. Such simple relation does not hold for the transverse susceptibility $\chi_{\perp}$ as M^x and H_0 do not commute.

The correlation functions $\rho_{x,z}$, computed according to the formula (3), are reported in Tables I and II for the ferromagnetic ($J>0$) and antiferromagnetic ($J<0$) interactions, respectively.

For the XY model ($\Delta=0.0$) ρ_z can be compared with the exact values[33] reported in the first column of Tables I and II. Above the reduced temperature $\tau=k_BT/|J|\simeq 0.15$, our extrapolated data do not deviate from the exact data more than 4%, whereas for $\tau\geq 1.0$ they coincide at least up to five significant digits. For the ferromagnetic isotropic Heisenberg model ($\Delta=1.0$) we find $\rho_x=\rho_z$ and the corresponding results can be compared with the high-temperature expansion data[34] denoted as χ_{HTS} in Table I. The latter are very well established with an error less than 1% at $\tau=0.5$ which increases to 10% as $T\rightarrow 0$. Thus our data up to $\tau=0.15$ are within these error bars. For both cases considered here, the extrapolated results are consistent with the previous data[33,34] up to $\tau=0.10$ but the accuracy is considerably decreased.

Our results can be compared with those of Bonner and Fisher[28] as far as ρ_z is concerned for the antiferromagnetic interactions. The latter have been extracted from the analysis of finite rings. An excellent agreement is found up to $\tau=0.25$ with the 4% error at that point for $\Delta=1$ and $\Delta=1/0.7$. Taking into account that in Ref. 28 the reduced susceptibility $\rho_z/4\tau$ is considered, we find the position of the maximum for $\Delta=1.0$ at $\tau=1.288$ with the corresponding height 0.073 47 whereas Bonner and Fisher report the value 0.073 46. Our estimate of the ground-state energy for the antiferromagnetic XY model is $-0.637J$ while the exact value[33] is $-0.6366J$.

Some results presented in Tables I and II will be referred to later on in order to make contact with experimental results on the susceptibility and the correlation length.

B. Correlation length results

In this section the inverse correlation length κ for the spin pair correlation functions

$$\rho_n^x=\langle\sigma_i^x\sigma_{i+n}^x\rangle , \quad \rho_n^z=\langle\sigma_i^z\sigma_{i+n}^z\rangle \tag{10}$$

is calculated. We refer to the following definitions[35] of the transverse and longitudinal inverse correlation lengths

$$\kappa_x=-\lim_{n\rightarrow\infty}\ln|\rho_{n+1}^x/\rho_n^x| ,$$
$$\kappa_z=-\tfrac{1}{2}\lim_{p\rightarrow\infty}\ln(\rho_{2p+3}^z/\rho_{2p+1}^z) . \tag{11}$$

In the definitions (11) the idea about the exponential decay of the correlation functions in the paramagnetic region and on distances much larger than the correlation lengths ξ is implemented. The definitions (11) lead, in the finite-size calculations, to the following problems. Not only the limits in (11) cannot be precisely taken but also the correlation function decreases by several orders of magnitude if $n\gg\xi$ so that the accuracy of the numerical computations becomes questionable even for finite n. Our numerical results can be reliable provided that the correlation length ξ is much smaller than N (the length of the chains) and the corresponding correlation functions do not fall off too rapidly. This is practically fulfilled if

TABLE I. The zero-field correlation functions $\rho_{x,z}$ of the longitudinal and transverse spin components for the ferromagnetic ($J>0$) interactions.

Δ		0.0		0.90		0.95		1.0		1.5	
k_BT/J	ρ_z^{ex}	ρ_x	ρ_z	ρ_x	ρ_z	ρ_x	ρ_z	$\rho_{x,z}$	χ_{HTS}	ρ_x	ρ_z
0.10	0.063 93	6.4	0.05	8.4	0.984	7.5	2.04	5.4	6.38	2.84	12.0
0.15	0.096 44	6.3	0.10	6.7	1.476	5.8	2.52	4.61	4.961	3.26	8.0
0.20	0.129 73	5.9	0.13	5.4	1.782	4.78	2.64	4.02	4.172 0	3.22	6.0
0.25	0.164 24	5.6	0.17	4.6	1.938	4.10	2.62	3.59	3.664 0	3.07	4.9
0.30	0.200 34	5.2	0.201	3.97	2.004	3.63	2.55	3.27	3.307 0	2.90	4.20
0.35	0.238 03	4.82	0.239	3.55	2.021	3.29	2.465	3.02	3.041 1	2.75	3.71
0.40	0.276 99	4.48	0.277	3.23	2.012	3.03	2.380	2.824	2.834 77	2.616	3.36
0.45	0.316 64	4.17	0.316 7	2.987	1.989	2.827	2.299	2.664	2.669 54	2.499	3.09
0.50	0.356 31	3.90	0.356 4	2.794	1.960 1	2.663	2.225	2.531	2.533 94	2.397	2.882
1.0	0.669 11	2.392	0.669 11	1.935 0	1.674 49	1.902 0	1.768 8	1.868 8	1.868 89	1.835 5	1.975 1
2.0	0.888 97	1.617 2	0.888 97	1.489 03	1.399 58	1.481 05	1.435 81	1.473 02	1.473 03	1.464 97	1.511 25
3.0	0.947 38	1.387 31	0.947 38	1.330 74	1.280 16	1.327 34	1.301 85	1.323 92	1.323 92	1.320 48	1.346 37
4.0	0.969 70	1.280 75	0.969 70	1.249 43	1.214 83	1.247 57	1.230 17	1.245 71	1.245 71	1.243 84	1.261 45
5.0	0.980 39	1.219 79	0.980 39	1.200 03	1.173 94	1.198 87	1.185 76	1.197 71	1.197 71	1.196 54	1.209 77
6.0	0.986 30	1.180 46	0.986 30	1.166 88	1.146 02	1.166 09	1.155 62	1.165 30	1.165 30	1.164 51	1.175 06

TABLE II. The zero-field correlation functions $\rho_{x,z}$ of the longitudinal and transverse spin components for the antiferromagnetic ($J<0$) interactions.

Δ		0.0		1.0	1.10		10.7
k_BT/J	ρ_z^{ex}	ρ_x	ρ_z	$\rho_{x,z}$	ρ_z	ρ_z	ρ_z
0.10	0.063 93	0.15	0.05	0.0	0.0	0.0	0.0
0.15	0.096 44	0.17	0.10	0.01	0.02	0.01	0.01
0.20	0.129 73	0.18	0.13	0.03	0.03	0.03	0.02
0.25	0.164 24	0.19	0.17	0.05	0.05	0.05	0.03
0.30	0.200 34	0.20	0.201	0.07	0.07	0.06	0.04
0.35	0.238 03	0.21	0.239	0.09	0.09	0.08	0.05
0.40	0.276 99	0.23	0.277	0.10	0.10	0.09	0.07
0.45	0.316 64	0.24	0.316 7	0.11	0.11	0.10	0.08
0.50	0.356 31	0.261	0.356 4	0.13	0.13	0.12	0.09
1.0	0.669 11	0.418 3	0.669 11	0.288	0.284	0.267	0.210
2.0	0.888 97	0.618 35	0.888 97	0.546 17	0.541 11	0.520 75	0.445 8
3.0	0.947 38	0.720 81	0.947 38	0.680 54	0.677 23	0.658 55	0.591 34
4.0	0.969 70	0.780 79	0.969 70	0.755 79	0.753 60	0.737 24	0.679 51
5.0	0.980 39	0.819 81	0.980 39	0.802 93	0.801 40	0.787 08	0.737 19

$\xi \ll N$ and $2\xi \leq n \leq 3\xi$. Owing to the peculiar behavior of ρ_n^z, one has to consider the distances n which are even in lattice unit so that the smallest values are $n_1=2$ and $n_2=4$. For chains considered here ($N=8-11$) $\xi<4$. If $\xi=3$, then we find $n_1=6$ and $n_2=8$ to fulfill the second condition so that we have a single pair (8,6) referring to the definition (11) of κ_z and we have no statistics. If $\xi=1$, then $n_1=2$, $n_2=4$, and $n_2>3\xi$ so that ρ_n^z is rapidly decreasing, and it will be difficult to proceed to $n=6$.

We conclude that our estimates of κ_z can be less accurate. However, the corresponding computations of the quantity κ_x are more successful and they are of physical interest.[8]

Our calculations of κ_x proceed in the following way. For a given chain we calculate all possible values ρ_n^x, where n ($\leq N-3$) is a constant, and then we find the corresponding mean value. The inverse correlation length κ_x is extracted from (11), where we put $3\leq n\leq N-4$. The values κ_x reported here are the corresponding extrapolated mean values calculated for all possible n and the error bars stand for the standard deviations. The quantity κ_z is evaluated in a similar way with some necessary modifications.

In Fig. 1 we present the results for the XY model. The exact results[35] are drawn in dashed lines whereas our estimates for κ_x and κ_z are reported by full circles and full squares, respectively. The inverse correlation length κ for the isotropic Heisenberg model ($\Delta=1.0$) is depicted in Fig. 1 by the solid line. Our estimates for κ_z, as expected, are less accurate. In order to consider the chains as long as possible, we report in this case the results for $N=11$. The deviations in κ_z found at the low-temperature region follow from the finite-size effects (κ_z^{-1} is comparable with N, whereas for $\tau>1$ they follow from the fast decay of the correlation functions). In that region $|\rho_{n=5}^z|<10^{-5}$ so that we calculate κ_z from the corresponding ratio (1) with $n=3$ and 1. This accounts for a jump of data for $\tau>1.25$.

Finally, we find rather good agreement with the exact data for κ_x in the reduced temperature region $\tau\geq 0.1$ and for κ_z, in the region $0.2\leq\tau\leq 1.2$, as far as the XY model is concerned.

It is worthwhile noticing that there is an ambiguity in the definition of the inverse correlation length κ. The alternative definition[36] is

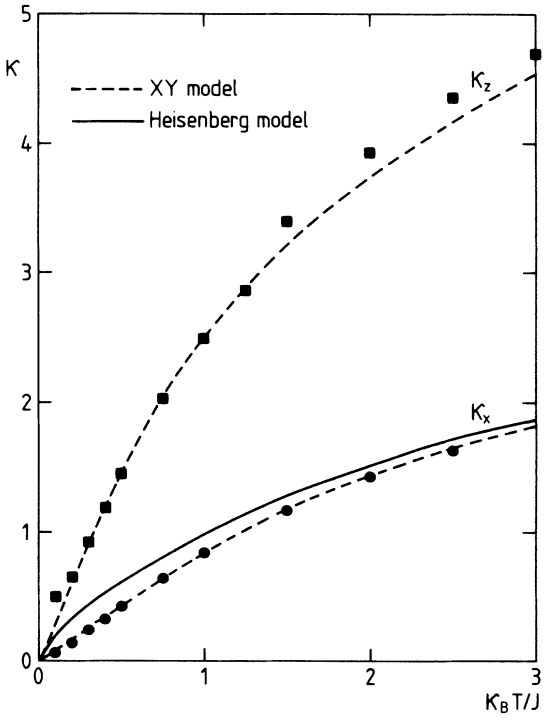

FIG. 1. Inverse correlation lengths κ of the transverse and longitudinal spin components vs k_BT/J in the case $J>0$. The dashed curves represent exact results for the XY model against our estimates for κ_x (in solid circles) and κ_z (in solid squares). The solid line depicts the extrapolated κ values for the isotropic Heisenberg model.

TABLE III. The transverse inverse correlation length κ_x for different values of anisotropy as a function of the reduced temperature k_BT/J.

$\frac{k_BT}{J}/\Delta$	0.0	0.95	1.0	0.0	0.95	1.0
0.1	0.06±0.05	0.14±0.03	0.20±0.06	0.05	0.06	0.08
0.2	0.14±0.06	0.28±0.03	0.32±0.05	0.10	0.17	0.20
0.3	0.24±0.04	0.39±0.03	0.42±0.03	0.17	0.29	0.32
0.4	0.32±0.03	0.49±0.02	0.52±0.02	0.26	0.41	0.43
0.5	0.42±0.02	0.59±0.01	0.61±0.02	0.36	0.52	0.54
0.75	0.64±0.01	0.80±0.01	0.81±0.01	0.61	0.77	0.79
1.0	0.836±0.008	0.979±0.008	0.992±0.008	0.84	0.99	1.01
1.5	1.16	1.27	1.28	1.22	1.37	1.38
2.0	1.42	1.50	1.52	1.54	1.67	1.69
2.5	1.63	1.70	1.71	1.81	1.94	1.95
3.0	1.81	1.86	1.87	2.05	2.18	2.19

$$\kappa_\alpha^2=\rho_\alpha/\left[\frac{1}{N}\sum_{ij}|i-j|^2\langle\sigma_i^\alpha\sigma_j^\alpha\rangle\right], \tag{12}$$

where ρ_α is defined in (2). This definition (hereafter referred to as II) is adopted in the transfer-matrix calculation[8] of κ in the classical limit. As some differences in κ were pointed out for the classical model,[36] we have also performed the calculations of the inverse correlation length κ_x by having recourse to (12). The results are given in the last three columns of Table III. In the first part of Table III the numerical data of κ_x, found from (11) and partially depicted in Fig. 1, are reported. The latter are supplemented by the corresponding standard deviations if they exceed 1%. The definition II leads to the values which are systematically smaller than those obtained from the definition I in the low-temperature region and systematically larger in the high-temperature region.

C. Susceptibility results

The longitudinal susceptibility $\chi_\parallel$ of the model (1) is related via (9) to the corresponding function ρ_z. The expression for the transverse susceptibility $\chi_\perp$ can be found from (4) if the magnetic field H is applied in the x direction so that

$$\hat{H}=H_0-mHM^x, \tag{13}$$

where H_0 and M^x are defined in (1) and (2), respectively, and $m=\frac{1}{2}g\mu_B$. Noncommutativity of H_0 and M^x becomes essential in the expansion (7) and leads to the following formula:

$$\chi_\perp=\frac{m^2}{Z_0}\left[\beta\sum_n e^{-\beta E_n}\langle n|M^x|n\rangle^2+\beta\sum_{n\neq k\ (E_m=E_k)} e^{-\beta E_n}|\langle n|M^x|k\rangle|^2+2\sum_{n\neq k\ (E_n\neq E_k)} e^{-\beta E_n}\frac{|\langle n|M^x|k\rangle|^2}{E_k-E_n}\right], \tag{14}$$

where Z_0 is the partition function of the Hamiltonian (1) and E_n, $|n\rangle$ stand for its eigenvalues and eigenvectors, respectively. In contrast to the usual expressions,[37] the diagonal matrix elements are present in (14) as we adapt the σ^x representation here. Defining the reduced susceptibility $\chi_N(T)$ per site as

$$\chi_N(T)=\frac{J}{Nm^2}\chi(T), \tag{15}$$

we immediately obtain for the reduced longitudinal susceptibility

$$\chi_N^\parallel(T)=\frac{J}{k_BT}\rho_z \tag{16}$$

and for the molar susceptibility

$$\chi^{\text{mole}}=m^2N_A\chi_N(T)/J, \tag{17}$$

where N_A is Avogadro's number.

We have performed the calculations of the reduced susceptibility $\chi_N^\perp(T)$ for the chains up to $N=10$ and we have extrapolated the results in $1/N$. The finite-size data are split for the antiferromagnetic interactions at low temperatures subject to an even or odd N. In that case we extrapolate separately N-even and N-odd data, and we take the average. Our results are presented explicitly in Table IV. We can compare the results for the antiferromagnetic XY model ($\Delta=0.0$) with those obtained from the closed rings and the Padé-approximant analysis.[37] Our linear-extrapolation procedure in $1/N$ is confirmed very well in this case. The results for the parameters $\Delta=0.95$ ($J>0$) and $\Delta=1.10$ ($J<0$) are reported in Table IV as they model some physical compounds and will be referred to in the next section.

TABLE IV. The zero-field reduced transverse susceptibility of the infinite chains extrapolated linearly in $1/N$ for various temperatures.

Δ	0.0	0.95	1.1
$k_BT/\|J\|$	$(J\leq 0)$	$(J\geq 0)$	$(J\leq 0)$
0.2	0.21	23.0	0.16
0.4	0.27	7.5	0.23
0.6	0.31	4.02	0.25
0.8	0.339	2.62	0.269
1.0	0.346	1.901	0.282
1.2	0.343 0	1.472	0.288 2
1.4	0.333 70	1.191	0.288 5
1.6	0.321 49	0.994 6	0.284 8
1.8	0.308 13	0.850 3	0.278 4
2.0	0.294 59	0.740 6	0.270 37
3.0	0.235 30	0.442 54	0.225 66

III. COMPARISONS AND CONCLUSIONS

We first discuss the comparison between the theoretical results and the measured experimental data for CHAB[8] and CDC.[9] In Fig. 2 the in-plane inverse correlation length κ_x/T (measured along CHAB-d14 chains)[8] is presented for the deuterated version of CHAB. The open circles are the experimental data extracted from the neutron-scattering profiles.[8] The theoretical predictions[8] for the classical Hamiltonian (1) with $\Delta=0.95$ are drawn in as the solid line. The corresponding curve has been found numerically by the transfer-matrix method choosing the spin length equal to $\frac{1}{2}$, instead of the semiclassical value $\sqrt{3/2}$. The latter would lead to the results reduced by a factor of 3. The exact result for the XY model is represented by a dotted line and reveals a linear dependence of κ on T at low temperatures.

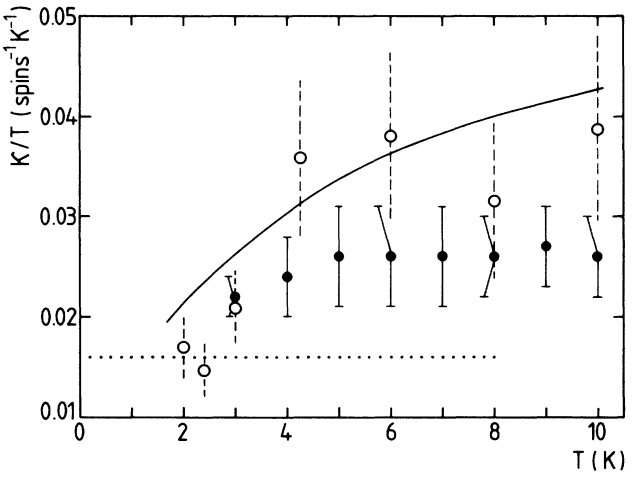

FIG. 2. Temperature dependence of the inverse correlation length κ, depicted as κ/T for the in-plane spin components. Experimental data along the CHAB-d_{14} chains are denoted by open circles with the error bars in the dashed lines. The theoretical estimates for the classical model are drawn by a solid line. Our estimates are given by solid circles with the error bars in solid lines. The exact results for the quantum XY model are depicted by the dotted line.

The experimental data show that the correlation length $\xi(T)$ increases from 2.5 at $T=10$ K and 6 at $T=4.5$ to 16.5 at 3 K. In the high-temperature part of the region considered experimentally we find the correlation length $\xi(=1/\kappa)$ to be small with respect to $N=10-11$, so that it seems possible to perform our calculations in that case. Our data are reported by solid circles together with the error bars from $T=10$ K down to $T=3$ K, where the correlation length exceeds the size of the chains considered here. On the basis of the test calculations performed for the XY model (Fig. 1) we believe that our data at low temperatures ($T<4.5$ K) at least represent the proper order of magnitude, the more so as the standard deviations are relatively small. Clearly, the experimental and the theoretical error bars overlap so that our data are consistent with the experimental findings. The theoretical values are systematically smaller than the experimental ones, however. Qualitatively, our results represent properly the experimental features: There is a plateau for $T>5$ K and a decrease of the data towards the XY value at low temperature (the crossover to the XY behavior). Our findings are below the classical ones. The same feature of the exact κ/T values and the corresponding classical counterparts have been found[8] for the XY model. It is likely that our values of κ_x for the anisotropic model with $\Delta=0.95$ underestimate the exact values as it is the case for the XY model (Fig. 1).

It is worthwhile emphasizing that the interpretation of the neutron-scattering experiments is not direct for the system considered here. The intensity profiles have been fitted by a single Lorentzian, assuming only one correlation length for the system. As κ_x and κ_z are different especially at low temperatures (e.g., Fig. 1), one has to estimate theoretically this difference and the corresponding susceptibilities χ_α, as the observed intensities are proportional to χ_α. In Fig. 3 we plot our estimates of $\chi_N^\perp/4J$ and $\chi_N^\parallel/4J$ in full lines whereas the corresponding estimates in the classical limit are drawn by the dashed lines. The quantum Monte Carlo[26] (QMC) data for $\chi_N^\perp/4J$ are reported by the full squares. The latter confirm rather well our estimates in the temperature range considered here. Below $\tau(\equiv k_BT/J)\simeq 0.15$ quantum effects in both $\chi_N^\parallel$ and $\chi_N^\perp$ become pronounced. As far as the inverse correlation length κ is concerned our data for κ_x (Table III) are close to those displayed for the isotropic model in Fig. 1, whereas $\kappa_z(T)\simeq 0.44-0.45(T<10$ K). Clearly, our results for χ and κ do not confirm the values found for their classical counterparts.[8] However, the quantum and classical ratios $\chi_N^\perp/\chi_N^\parallel$ and κ_x/κ_z have the same order of magnitude so that the arguments[8] underlying the interpretation are confirmed. The main point is that in the region where $\kappa_z \gg \kappa_x$, $\chi_N^\parallel \ll \chi_N^\perp$ so that the intensity originating from the longitudinal spin components can be neglected, whereas for $T>8$ K, $\kappa_z/\kappa_x \simeq 1.1$ and the systematic error following from the assumption $\kappa_z=\kappa_x$ is of the same order as the experimental uncertainty. In any case the experimental inverse correlation length κ is not exactly κ_x but a value somehow averaged. It is likely that

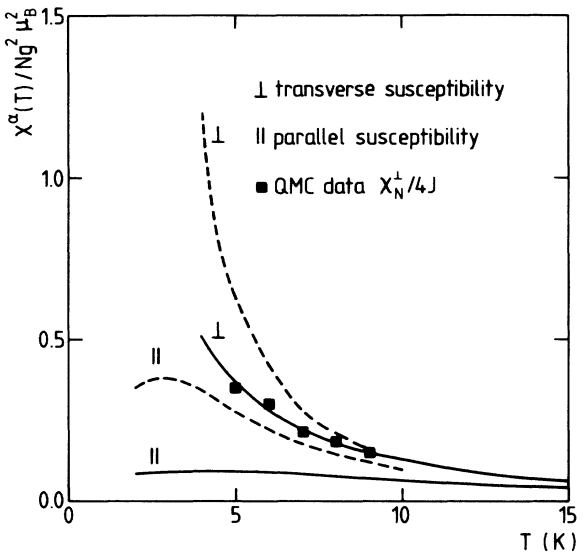

FIG. 3. Temperature dependence of the susceptibility $\chi_N^{\alpha}/4J=\chi^{\alpha}(T)/Ng^2\mu_B^2$ for the model with $J/k_B=55$ K and $\Delta=0.95$. The full lines represent our results and the dashed curves represent the corresponding susceptibilities for the classical spins (after Ref. 8). The solid square denotes the quantum Monte Carlo esimates of $\chi_N^{\perp}/4J$ (after Ref. 26).

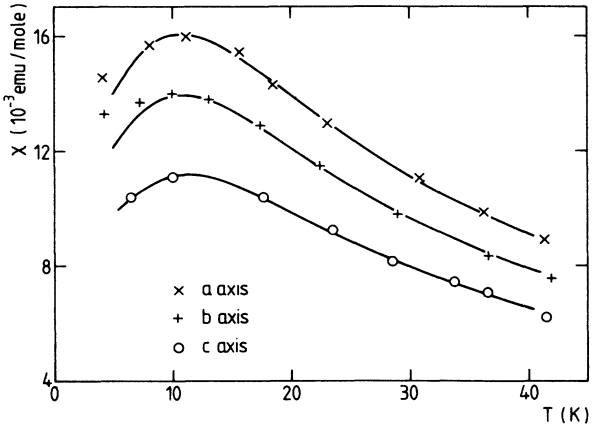

FIG. 4. Temperature dependence of the single-crystal susceptibilities for the deutered version of CDC (reported by crosses and circles) and our theoretical estimates drawn by solid lines. The experimental data are fitted for the following parameters: $J/k_B=-8.25$, $\Delta=1.1$ and $g_a=2.21$, $g_b=1.89$, $g_c=2.06$.

$\kappa>\kappa_x$ as $\kappa_z>\kappa_x$. Taking this into account, the ambiguity in the definition itself and the accuracy of our extrapolations, we conclude that we get at least a semiquantitative agreement with experiment.

Finally, we make contact with the recent susceptibility data on CDC[9] which is found to be an easy-axis spin-$\frac{1}{2}$ antiferromagnet described by the Hamiltonian (1) with the following parameters: $J/k_B=-8.25$ and $\Delta=1.10$. Our parallel susceptibility data have been found from the analysis of the chains up to $N=11$ and the transverse-susceptibility data for N up to 10. We do not recover the agreement between the experimental molar susceptibilities and the theoretical estimates for the g parameters quoted in Ref. 9. We find that the previous estimates[9] are underestimated by 6–7% as far as the transverse-susceptibility data are concerned (a-axis and c-axis data) and are underestimated by 9–10% for the parallel susceptibility (b-axis data). The differences cannot be associated with the accuracy as for $J/k_B=-8.25$, the calculations are reliable in the reported range of temperatures ($T>5$ K), and the error is less than 1% for $T>10$ K. They cannot be associated with different unit conventions as we find different proportionality constants for the easy-axis data and for the hard-plane data.

We can fit our results to the experimental findings very easily if we rescale the values of the corresponding g factors with respect to those quoted before. After rescaling, the g factors are somewhat reduced. For the fit presented in Fig. 4 we find $g_a=2.21$, $g_c=2.06$, and $g_b=1.89$ which should be compared with the experimental EPR[38] values 2.30, 2.10, and 2.02, respectively.

In Fig. 4 we present only some arbitrarily chosen experimental points fully reported in Ref. 9. Apparently, the fit is surprisingly good with the parameters $J(=-8.25)$ and $\Delta(=1.10)$ found previously[9] and somewhat rescaled g factors which are still consistent with those found from the EPR experiment.

In conclusion, we have reported extrapolated finite-size calculations of the correlation functions, correlation length, and susceptibility by having recourse to the quantum spin statistics. We have compared them with the existing theoretical estimates for some values of the parameters J and Δ as well as we have made contact with recent experimental data on CHAB and CDC. Our results support previous interpretations of CHAB as the quasi-one-dimensional spin-$\frac{1}{2}$ easy-plane ferromagnet and CDC as the corresponding easy-axis antiferromagnet.

Finally, we comment on the extrapolation procedure. The results reported here are found by the linear extrapolation in $1/N$. We tried to apply the least-square fit up to $(1/N)^2$, but it seems that the linear extrapolation gives better overall representation, and we found nonsatisfactory estimates from the Padé-approximant analysis.[37] The corresponding estimates from different Padé approximants (when applicable) oscillate with increasing temperature, contrary to our estimates from linear extrapolations. It is likely that the previous[37] successful Padé analysis of the susceptibility series for the antiferromagnetic XY model is applicable for the closed rings only. For our open chains we cannot repeat the Padé-approximant analysis for the XY model as we do not find the monotonously increasing sequence of data for successive values of N. The features are temperature dependent. We emphasize, however, that the Padé-approximant results[37] for the XY model can be recovered within our linear-extrapolation procedure (Table IV).

ACKNOWLEDGMENTS

I would like to thank Professor R. Dekeyser for many discussions, his help in the extrapolation analysis, and

perceptive comments on the manuscript; Professor W. J. M. de Jonge and Dr. K. Kopinga for fruitful discussions on the experimental foundation of CHAB; Dr. A. Komoda for encouragement in Padé-approximant analysis. The discussions with Dr. C. Vanderzande and partial support from the Institute of Physics, Lodz University (under Polish Academy of Sciences Grant No. CPBP-01-08) are also acknowledged.

---

*Permanent address: Instytut Fizyki, Uniwersytet imienia Adama Mickiewicza, PL-60-769 Poznań, Poland.

[1]M. Steiner, J. Villain, and G. G. Windsor, Adv. Phys. **25**, 87 (1976); M. Steiner, in *Physics in One Dimension*, edited by J Bernasconi and T. Schneider (Springer-Verlag, Heidelberg, 1981).

[2]*Magnetic Excitations and Fluctuations*, edited by S. W. Lovesey, U. Balucani, F. Borsa, and V. Tognetti (Springer-Verlag, Heidelberg, 1984).

[3]F. Borsa, Phys. Rev. B **25**, 3430 (1982).

[4]M. Steiner, K. Kakurai, and J. K. Kjems, Z. Phys. B **53**, 117 (1983).

[5]K. Kopinga, A. M. S. Tinus, and W. J. M. de Jonge, Phys. Rev. B **25**, 4685 (1982).

[6]K. Kopinga, A. M. S. Tinus, and W. J. M. de Jonge, Phys. Rev. B **29**, 28 (1984).

[7]H. A. Groenendijk, H. W. J. Blöte, A. J. van Duyneveldt, R. M. Gaura, C. P. Landee, and R. D. Willet, Physica B **106**, 47 (1981).

[8]K. Kopinga, W. J. M. de Jonge, M. Steiner, G. C. de Vries, and E. Frikkee, Phys. Rev. B **34**, 4826 (1986).

[9]C. P. Landee, A. C. Lamas, R. E. Greeny, and K. G. Bücher, Phys. Rev. B **35**, 228 (1987).

[10]A. C. Phaff, C. H. W. Swüste, W. J. M. de Jonge, R. Hoogerbeerts, and A. J. van Duyneveldt, J. Phys. C **17**, 2583 (1984).

[11]K. Kopinga, A. M. C. Tinus, W. J. M. de Jonge, and G. C. de Vries, Phys. Rev. B **36**, 5398 (1987).

[12]E. Magyari and H. Thomas, J. Phys. C **15**, L333 (1982).

[13]A. M. C. Tinus, W. J. M. de Jonge, and K. Kopinga, Phys. Rev. B **32**, 3154 (1985).

[14]T. Schneider and E. Stoll, Phys. Rev. B **22**, 5317 (1980).

[15]M. Fowler and X. Zotos, Phys. Rev. B **25**, 2806 (1982).

[16]M. Imada, K. Hida, and M. Ishikawa, J. Phys. C **16**, 35 (1983).

[17]T. Tsuzuki, Prog. Theor. Phys. **70**, 975 (1983).

[18]M. Moraldi, A. Rettori, and M. G. Pini, Phys. Rev. B **31**, 1971 (1985).

[19]R. Giachetti and V. Tognetti, Phys. Rev. Lett. **55**, 912 (1985); Phys. Rev. B **33**, 7647 (1986).

[20]M. D. Johnson and N. F. Wright, Phys. Rev. B **32**, 8798 (1985).

[21]H. C. Fogedby, K. Osano, and H. J. Jensen, Phys. Rev. B **34**, 3462 (1986).

[22]H. J. Mikeska and H. Frahm, J. Phys. C **19**, 3203 (1986).

[23]O. G. Mouritsen, H. Jensen, and H. C. Fogedby, Phys. Rev. B **30**, 498 (1984); H. J. Jensen, O. C. Mouritsen, H. C. Fogedby, and H. Hedegaard, *ibid.* **32**, 3240 (1985).

[24]M. G. Pini and A. Rettori, Phys. Rev. B **29**, 5246 (1984).

[25]F. Boersma, K. Kopinga, and W. J. M. de Jonge, Phys. Rev. B **23**, 186 (1981).

[26]I. Satija, G. Wysin, and A. R. Bishop, Phys. Rev. B **31**, 3205 (1985); G. M. Wysin and A. R. Bishop, *ibid.* **34**, 3377 (1986).

[27]G. Kamieniarz and C. Vanderzande, Phys. Rev. B **35**, 3341 (1987).

[28]J. C. Bonner and M. E. Fisher, Phys. Rev. **135**, A640 (1964).

[29]H. W. J. Blöte, Physica B **79**, 427 (1975).

[30]J. J. Cullen and D. P. Landau, Phys. Rev. B **27**, 297 (1983).

[31]H. Betsuyaku, Prog. Theor. Phys. **73**, 319 (1985).

[32]M. Suzuki, Prog. Theor. Phys. **56**, 1454 (1976).

[33]S. Katsura, Phys. Rev. **127**, 1508 (1962).

[34]G. A. Baker, G. S. Rushbrooke, and H. E. Gilbert, Phys. Rev. **135**, A1272 (1964).

[35]T. Tonegawa, Solid State Commun. **40**, 983 (1981).

[36]J. M. Loveluck, S. W. Lovesey, and S. Aubry, J. Phys. C **8**, 3841 (1975).

[37]P. M. Duxbury, J. Oitmaa, M. N. Barber, A. van der Bilt, K. O. Joung, and R. L. Carlin, Phys. Rev. B **24**, 5149 (1981).

[38]T. R. Reddy and R. Srinivsan, J. Chem. Phys. **45**, 2714 (1966).